

Supporting Information

A Rechargeable Al-N₂ Battery for Energy Storage and Highly Efficient N₂ Fixation

Ying Guo,^a Qi Yang,^a Donghong Wang,^a Hongfei Li,^b Zhaodong Huang,^a Xinliang Li,^a
Yuwei Zhao,^a Binbin Dong,^c Chunyi Zhi^{a,d*}

^aDepartment of Materials Science and Engineering, City University of Hong Kong, 83
Tat Chee Avenue, Kowloon, Hong Kong 999077, China

^bSongshan Lake Materials Laboratory, Dongguan, Guangdong 523808, China

^c National Engineering Research Center for Advanced Polymer Processing
Technology, Zhengzhou University, Zhengzhou, Henan 450002, China

^d Centre for Functional Photonics, City University of Hong Kong, Kowloon, Hong
Kong

Corresponding author: Prof. Chunyi Zhi

Email: cy.zhi@cityu.edu.hk

S1. Experimental section

Chemicals

Sodium tetrachloropalladate(II) (Na_2PdCl_4 , 98%), sulfuric acid (H_2SO_4 , 98%), deuterium oxide (D_2O , 99.9 atom % D), hydrochloric acid (HCl , 37%), graphene oxide (99%), sodium hydroxide (NaOH , > 98%), sodium hypochlorite solution (NaClO , available chlorine 4.0 %), p-Dimethylaminobenzaldehyde ($\text{C}_9\text{H}_{11}\text{NO}$), salicylic acid ($\text{C}_7\text{H}_6\text{O}_3$, 99%), hydrogen peroxide (H_2O_2 , 30%), trisodium citrate ($\text{C}_6\text{H}_5\text{Na}_3\text{O}_7$, 98%), sodium nitroferricyanide dehydrate ($\text{C}_5\text{FeN}_6\text{Na}_2\text{O} \cdot 2\text{H}_2\text{O}$, 99%), 2-propanol ($\text{C}_3\text{H}_8\text{O}$, 99.5%), aluminum chloride (AlCl_3 , 99.99%), N-(1-naphthyl) ethylenediamine dihydrochloride ($\text{C}_{12}\text{H}_{14}\text{N}_2 \cdot 2\text{HCl}$, 98%), and 1-butyl-3-methylimidazolium chloride ($\text{C}_8\text{H}_{15}\text{ClN}_2$, 97%) were purchased from Shanghai Macklin Biochemical Co., Ltd. N_2 gas (99.999 % purity) and Ar gas (99.999 % purity) were supplied by Linde HKO Ltd. W1S1005 carbon cloth was purchased from Fuel Cell Store Ltd.

Synthesis of graphene/Pd catalyst

50 mg graphene oxide was dispersed in 50 mL deionized water to achieve a yellow brown solution after the ultrasonic dispersion for 30 min. Then, the above graphene oxide solution and 1 mL 10 mM N_2PdCl_4 solution were transferred into a 100-mL vial under ultrasonic treatment for 2 h in an ice bath. Consequently, the mixture was washed with deionized water for several times and then the as-obtained product was frozen in liquid nitrogen and freeze-dried for 24 h.

The dried mixture was placed in a ceramic boat and heated at 200°C in Ar atmosphere

for 30 min with a ramp rate of 2°C. And then, the temperature was heated to 600°C with a ramp rate of 5°C for 4 h.

Pre-treatment of carbon cloth (CC) electrode

Firstly, CC was treated in 30 wt% H₂O₂ solution at 80°C for 1 h and consequently in 100 mL 5 M H₂SO₄ solution for 6 h at room temperature to remove residuals. Then, CC was washed with deionized water for 3 times and dried in a vacuum oven.

Characterization

The crystalline, morphologies and structures of the catalyst, electrode and nitrogen fixation and evolution products were investigated by X-ray Powder Diffractometer (XRD) using BRUKER SRD-D2 Phaser with Cu K α irradiation ($\lambda = 1.54 \text{ \AA}$), field-emission scanning electron microscopy (SEM, FEI Quanta 450 FEG) and JEOL-2001F field-emission TEM (JEOL-2001F). Raman spectra were collected under Renishaw in Via confocal Raman microscope with a 633 nm laser. The surficial chemical states and compositions of the as-obtained products were investigated by Scanning Auger and XPS (PHI Model 5802). ¹H-NMR measurements were performed on Bruker 600MHz ASCEND AVANCE III HD Nuclear Magnetic Resonance System (NMR-600). UV-vis spectroscopy measurements were carried out using a UV/VIS Spectrometer Lambda 2S. Before NMR tests, pH of the solutions was adjusted to 3 with 0.05 M H₂SO₄ and 0.1 M NaOH.

Preparation of graphene/Pd/CC cathode

Firstly, 5 mg of the as-synthesized graphene/Pd catalyst was dispersed in 1 mL mixture solution containing 2-propanol, deionized water and 5 wt.% Nafion solution (10:10:1)

and ultrasonic treatment for 30 mins. After that, homogenous catalyst ink was dropped on CC with the total load mass of 0.4 mg/cm². Then, it was dried at 40°C in a vacuum oven for 24 h. The available area of graphene/Pd/CC used for the Al-N₂ battery is 1 cm².

Assembly of Al-N₂ battery and electrochemical test

The home-made Al-N₂ battery (Figure S1) was assembled in glove box filled with Ar where the content of O₂ and H₂O was lower than 0.1 ppm, the pristine CC or graphene/Pd/CC electrode and the polished Al plate with 0.2 mm of thickness were used as cathode and anode, respectively. 1.5-mL solution consisting of aluminum chloride/1-butyl-3-methylimidazolium chloride (weight ratio = 1.3:1) was used as electrolyte for the Al-N₂ battery. The electrolyte was heated at 100°C for 30 min in glove box filled with Ar to remove residual water before it was applied to the battery. Before the Al-N₂ cell, the feeding gases were pre-purified by passage through the sealed trap (5 mL) containing anhydrous aluminum chloride and ion liquid electrolyte to remove the possible impurities from the feeding gases, N₂ or Ar flow with a flow rate of 20 mL/min was introduced into the battery cavity for 30 min to remove residual gas. The charge-discharge polarization curves were obtained under flowing N₂ gas (99.999 % purity) or Ar gas (99.999 % purity) on Land 2001A battery system at room temperature. Cyclic voltammograms (CV) tests were conducted at a voltage sweep rate of 0.05 mV/s on the electrochemical workstation (CHI 760E, Chenhua, China). For the morphological, structural and compositional characterizations, the resultant electrodes were subsequently rinsed in propylene carbonate, acetone, and ethanol to remove

residual electrolyte as much as possible and then were dried under vacuum at 40°C.

Electrochemical NRR test

Preparation of the working electrode for the aqueous NRR.

80 μ L of catalyst ink was dropped onto CC (1 cm \times 1cm) with 0.4 mg/cm² of the loading mass and followed by drying at 40°C in an oven.

Aqueous NRR measurements.

All NRR tests were performed in a three-electrode configuration with the CHI 760E workstation under ambient condition. A Pt wire and Ag/AgCl (3.0 M KCl) electrode were used as the counter and reference electrodes, respectively. The 1 cm \times 1 cm CC with graphene/Pd catalyst (loading mass is 0.4 mg/cm²) was used as the working electrode. All potentials reported for NRR test were given versus RHE, $E(\text{RHE}) = E(\text{Ag/AgCl}) + 0.059 \times \text{pH} + 0.222$.

Prior to NRR tests, the feeding gases were pre-purified by passage through an acidic trap (0.05 M H₂SO₄) and drying tube to remove any possible sources of N contamination and water gas. For aqueous NRR experiments, the electrolyte with 0.05 M H₂SO₄ saturated with N₂ for 30 mins at the flow rate of 20 mL/min. The chronoamperometry test was conducted at fixed potentials in N₂ or Ar-saturated 0.05 M H₂SO₄ solution (40 mL). All polarization curves were steady state after 10 CV cycles.

Quantitative determination of the products from nitrogen fixation.

The produced NH₃ was determined by using indophenol blue method (*Nature Mater.* **2013**, 12, 836). First, calibration curve was built by UV-Vis absorption spectra derived

from a series of 0.1 M NaOH solutions containing the given concentrations of $(\text{NH}_4)_2\text{SO}_4$. The NH_3 generated was carefully controlled to rule out possible contaminations according to the reported work (*Nature*, **2019**, 570, 504-508)

The quantity of NH_3 produced from the aqueous NRR.

2 mL electrolyte was taken out after NRR test, and 1.25 mL of solution consisting of 0.625 M NaOH, 0.36 M salicylic acid, and 0.17 M sodium citrate was added, and then 150 μL of sodium nitroferrocyanide solution (10 mg/mL) and 75 μL of NaClO solution with available chlorine 4.0 wt.% was added. After 2 h at ambient conditions, the UV-Vis absorption spectrum was recorded, and the absorbance value was obtained at the wavelength of 658 nm.

The quantity of NH_3 derived from the hydrolysis of the cathodic AlN product ($\text{AlN} + \text{NaOH} + \text{H}_2\text{O} = \text{NaAlO}_2 + \text{NH}_3$). The discharged cathode and electrode totally taken from Al- N_2 battery after electrochemical test were soaked in 20-mL 0.1 M NaOH aqueous solution in an ice bath. After the solution was diluted by 10 times with 0.1 M NaOH solution, then the quantity of NH_3 generated from the chemical reaction was determined by the above procedures. Finally, the quantity of NH_3 was determined by subtracting the background absorbance of 1.5-mL ionic liquid electrolyte.

Colorimetric detection of NO_3^- . First, a 5-mL solution was taken out from the cell. Then 0.10 mL of 1.0 M HCl solution was added into the above solution. After shaking for 10 min and standing for 5 min, the absorbance of NO_3^- was measured by using UV-Vis spectrophotometer at a wavelength range from 300 nm to 200 nm. The final absorbance of NO_3^- was calculated based on the absorbance value difference at

220 nm and 275 nm. The standard calibration curve can be obtained by the absorbance of the different known concentrations of NaNO₃.

Colorimetric detection of NO₂⁻. First, 5 mL of standard or electrolyte was added to the test tubes and followed by adding 0.10-mL solution containing 2.0 M HCl and 10 mg/mL sulfanilamide. After mixing and standing for 10 min, 0.10 mL of N-(1-Naphthyl) ethylenediamine dihydrochloride solution (10 mg/mL) was added into the above solution. After shaking and standing for 30 min, the absorbance of NO₂⁻ was measured by using UV-Vis spectrophotometer at a wavelength range from 650 nm to 450 nm. The final absorbance of NO₃⁻ was calculated at 540 nm. The standard calibration curve can be obtained by the absorbance of the different known concentrations of NaNO₂.

Faradaic efficiency (FE) and ammonia yield rate. FE and mass-normalized yield rate of NH₃ were calculated:

$$FE = (3F \times C \times V) / Q$$

$$\text{Yield rate} = 17C \times V / (t \times m)$$

Where F is the Faraday constant (96485 C/mol), C is the measured NH₃ concentration, V is the volume of electrolyte, Q is the total charge passed through the electrode and m is the loading mass of catalyst (0.4 mg).

S2. Figures and tables.

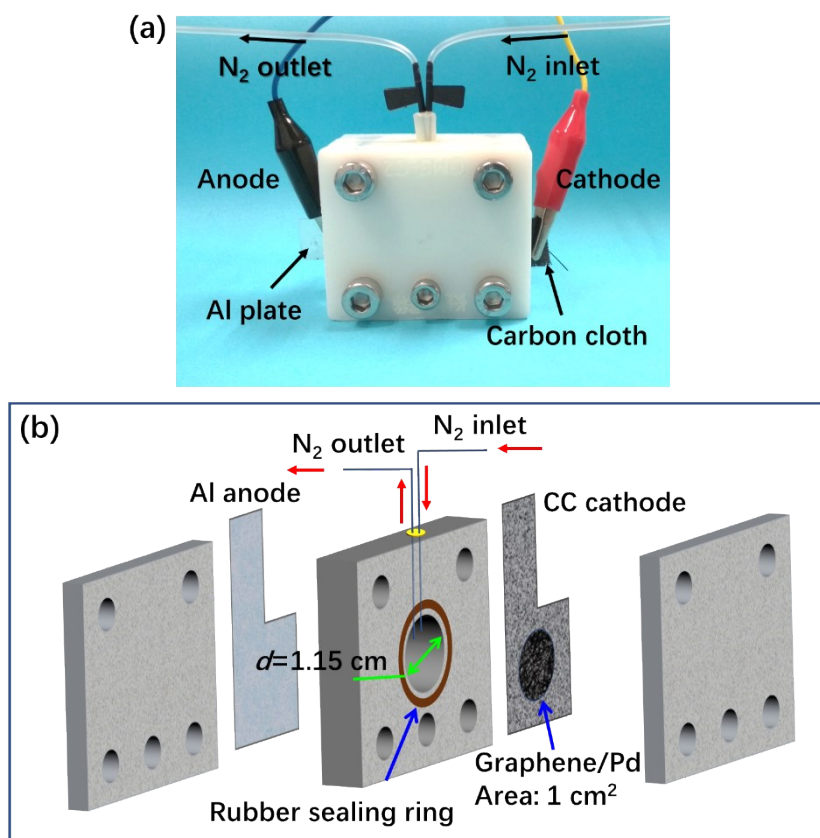


Figure S1. (a) photograph and (b) construction of the home-made polypropylene Al-N₂ battery configuration.

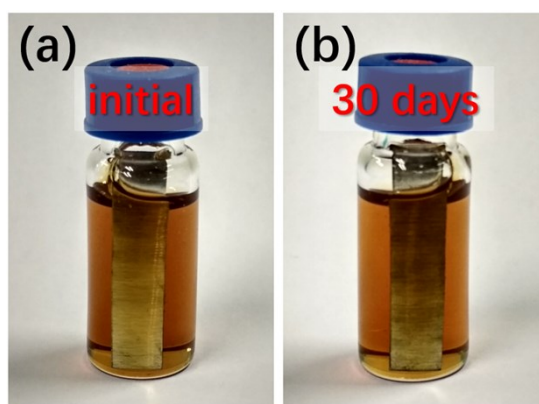


Figure S2. The stability test of Al plate in ionic liquid electrolyte.

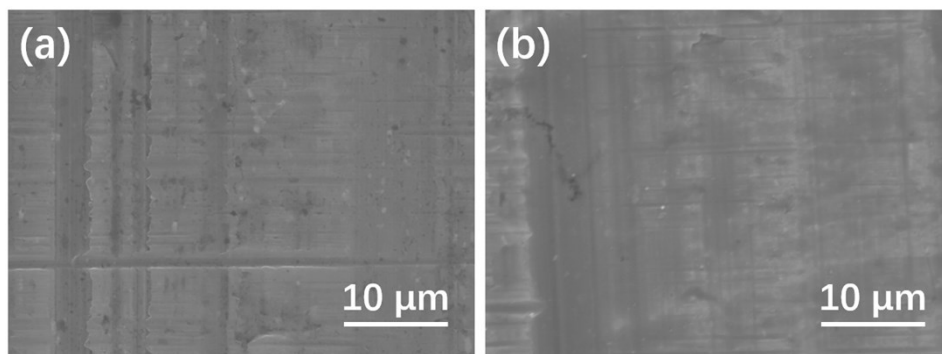


Figure S3. SEM images of (a) the initial Al plate and (b) Al plate after 30-day stability test.

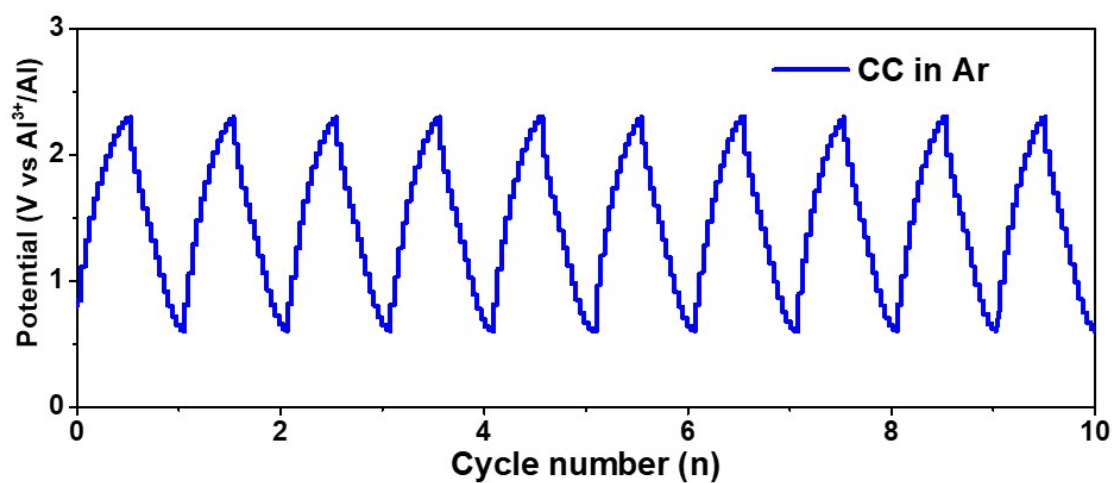


Figure S4. Cyclic performance of the Al-N₂ battery at 0.1 mA/cm² in Ar atmosphere.

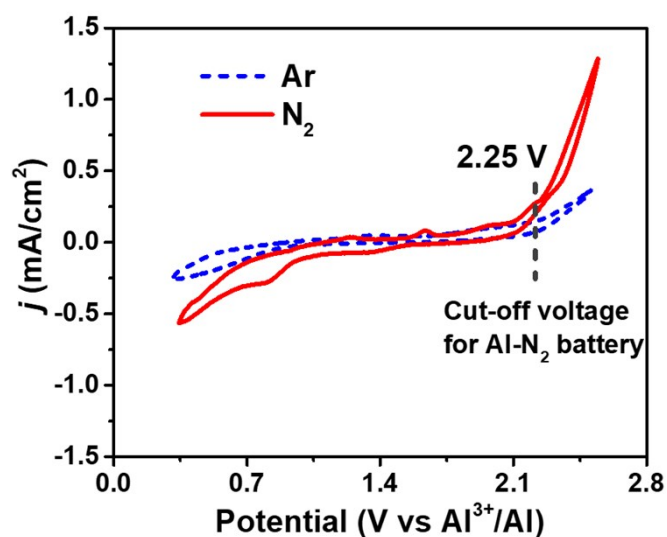


Figure S5. The large-window cyclic voltammetry curve of the Al-N₂ battery with the CC electrode at 0.05 mV/s in the N₂ and Ar atmospheres.

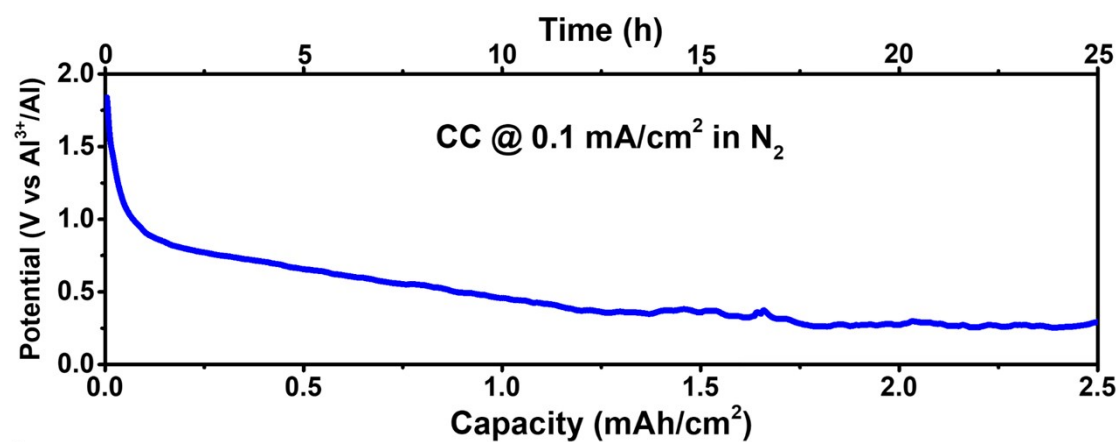


Figure S6. Deep discharging test of an Al-N₂ battery with the pristine CC electrode in the N₂ atmosphere for 25 h.

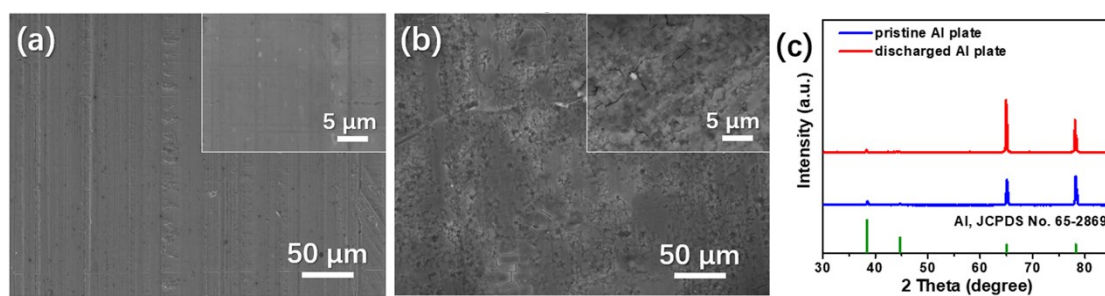


Figure S7. SEM images of (a) the pristine Al plate and (b) the discharged Al plate and their corresponding XRD patterns (c). It is noted that both Al anodes exhibit the intensity mismatch with the reference intensity, which can be attributed to the preferred orientation because of the plate-like shape (thickness is 0.2 mm), creating a systematic error in the observed diffraction peak intensities.

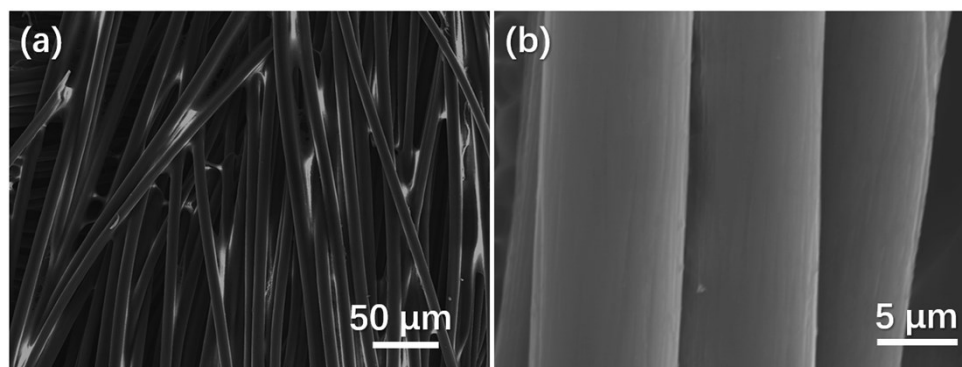


Figure S8. SEM images of the pristine CC.

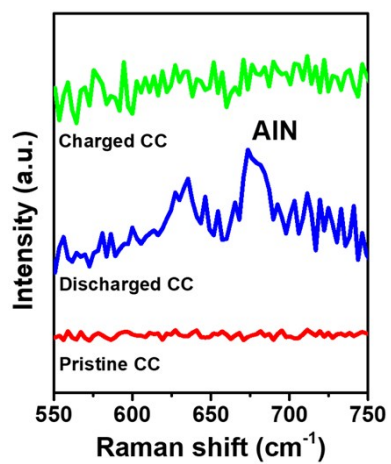


Figure S9. Raman spectra of the charged/discharged CC electrode and pristine CC.

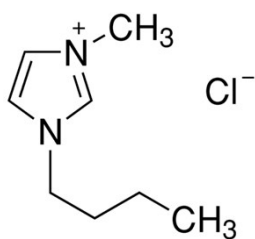


Figure S10. Chemical structure of 1-butyl-3-methylimidazolium chloride.

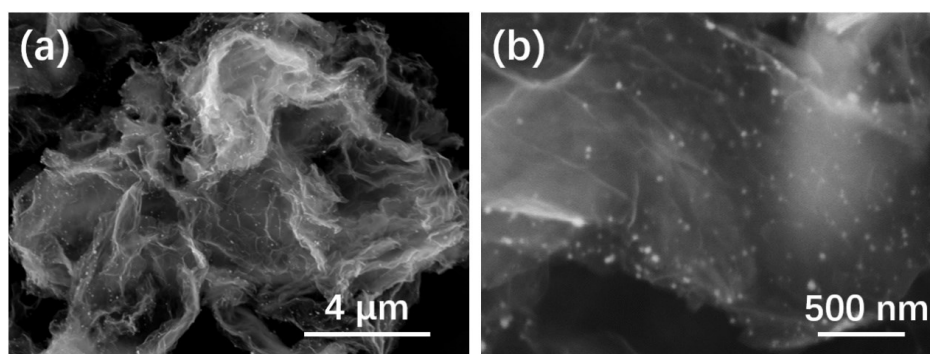


Figure S11. SEM images of graphene/Pd cathode catalyst.

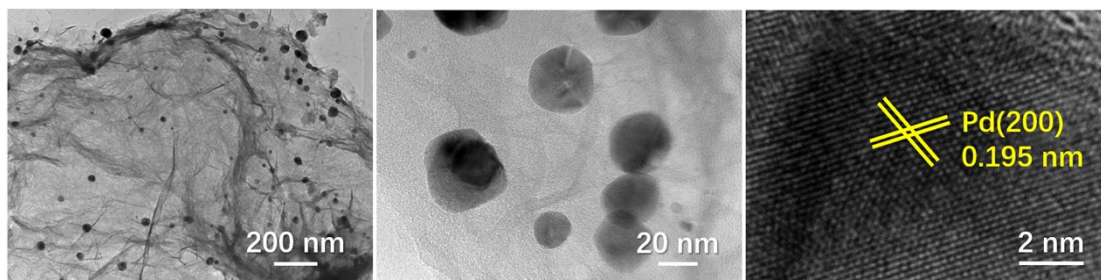


Figure S12. TEM images (a-b) and HRTEM image (c) of graphene/Pd cathode catalyst.

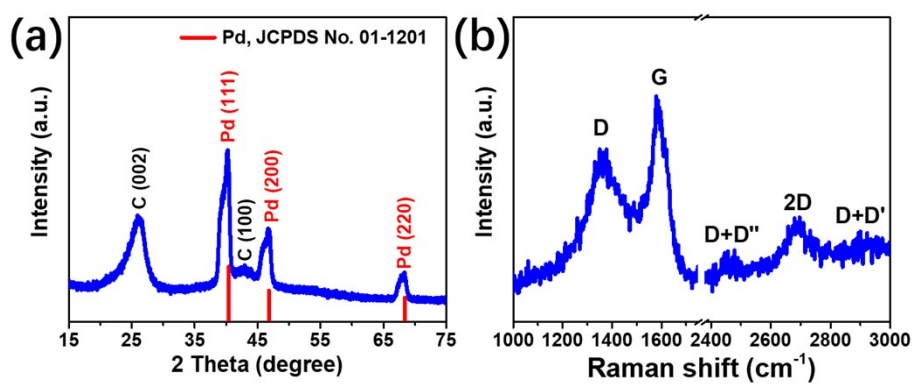


Figure S13. XRD pattern (a) and Raman spectrum (b) of graphene/Pd cathode catalyst.

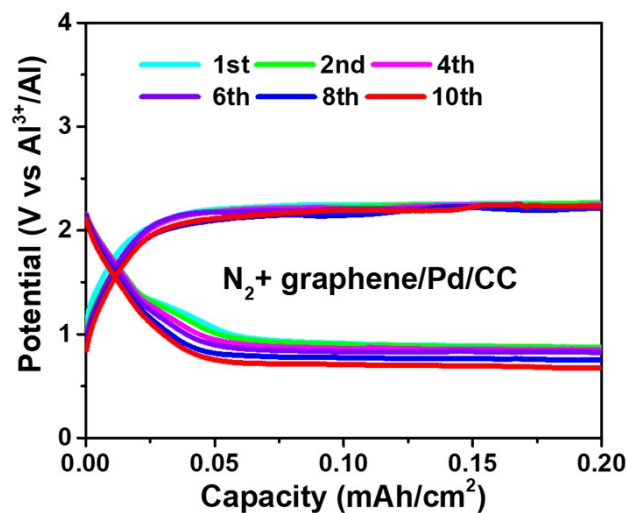


Figure S14. The charge/discharge curves of the Al-N₂ battery using graphene/Pd/CC as cathode against the cycle number.

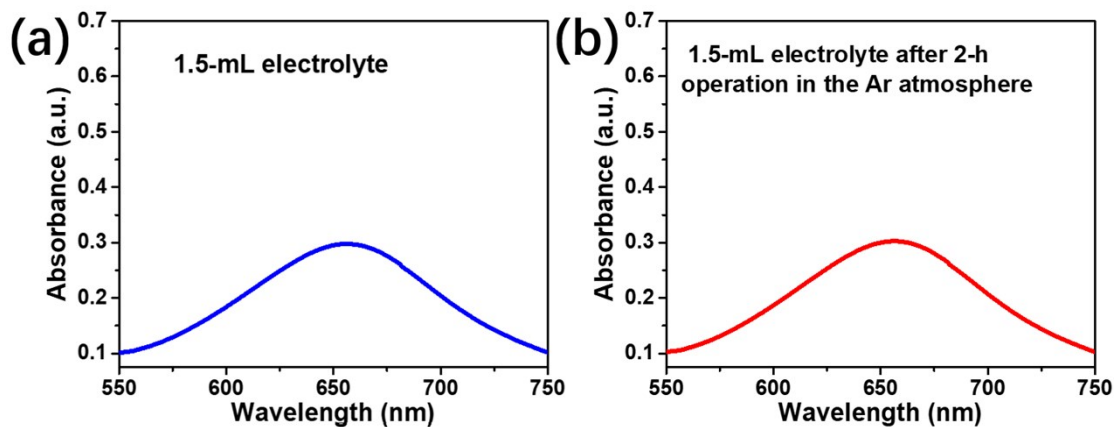


Figure S15. Control experiments of UV-vis spectra to verify the N₂ fixation obtained by the Al-N₂ battery in N₂ atmosphere.

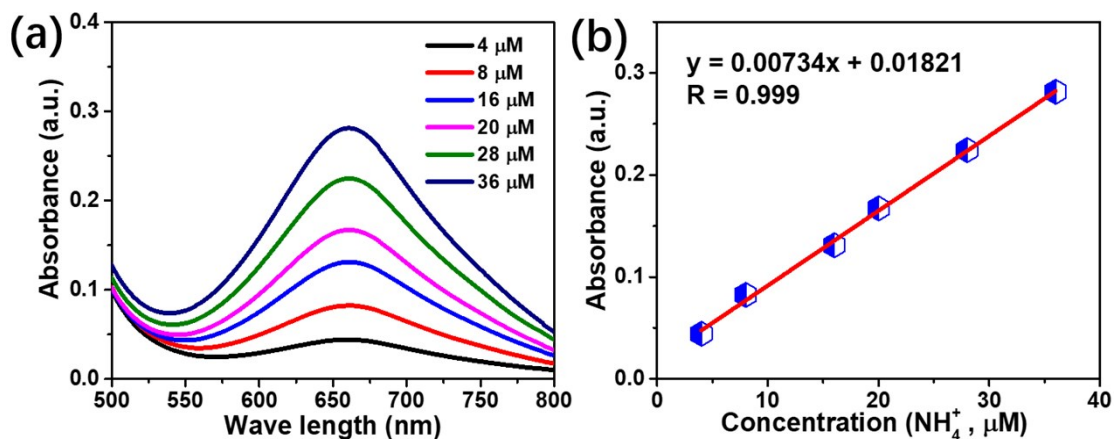


Figure S16. (a) The UV-Vis absorption spectra and (b) concentration-absorbance calibration curve of 0.1 M NaOH solution with a series of standard concentration of NH_4^+ using the indophenol blue method.

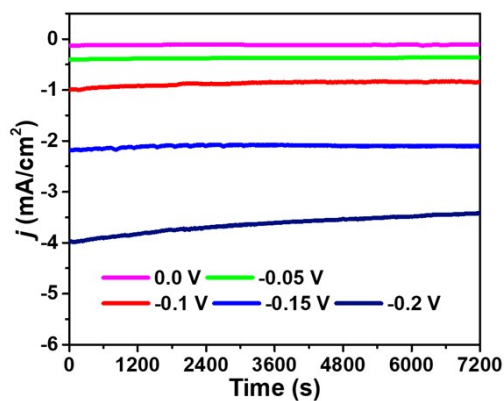


Figure S 17. Current-time profiles obtained at various potentials for calculating the whole charge quantity consumed.

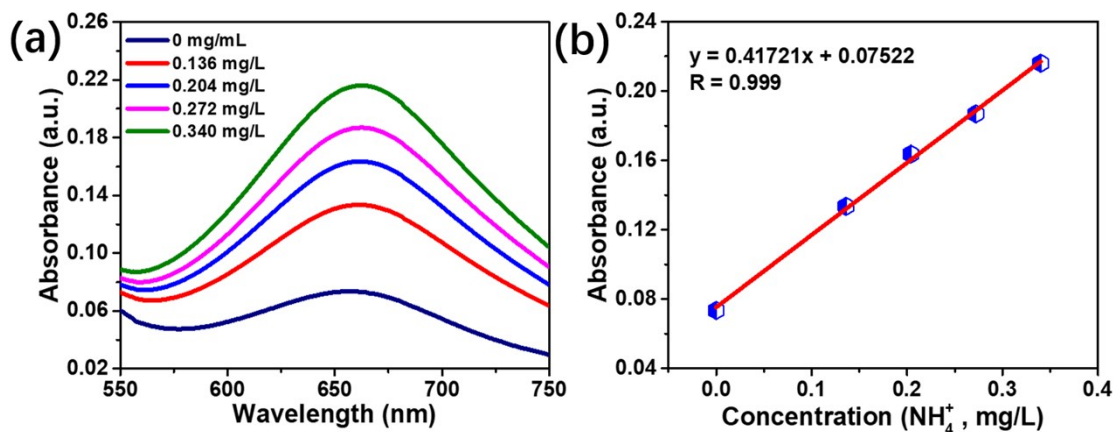


Figure S18. (a) The UV-Vis absorption spectra and (b) concentration-absorbance calibration curve of 0.05 M H_2SO_4 solution with a series of standard concentration of NH_4^+ using the indophenol blue method.

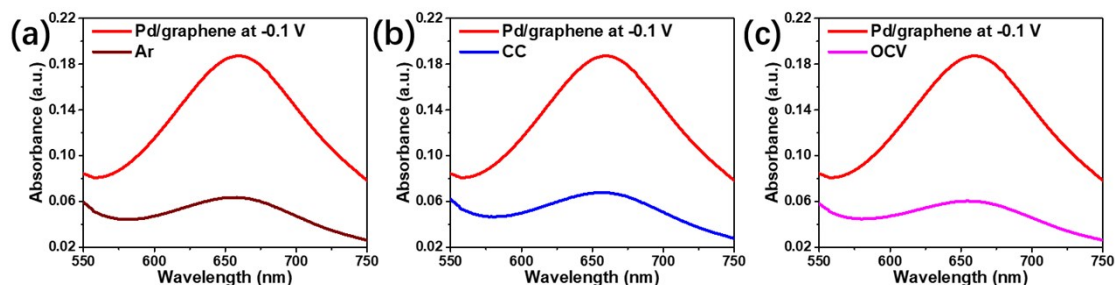


Figure S19. Control experiments to verify the electrochemical N_2 reduction catalyzed by graphene/Pd in N_2 -saturated 0.05 M H_2SO_4 aqueous solution.

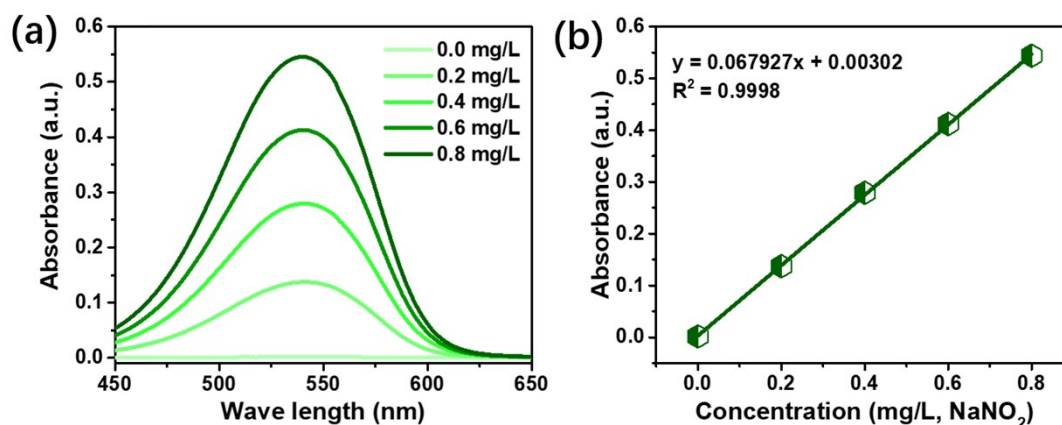


Figure S20. Calibration for nitrite determination. (a) UV-vis spectra for various concentrations of NaNO_2 . (b) Calibration curve used for calculating the concentration of nitrite.

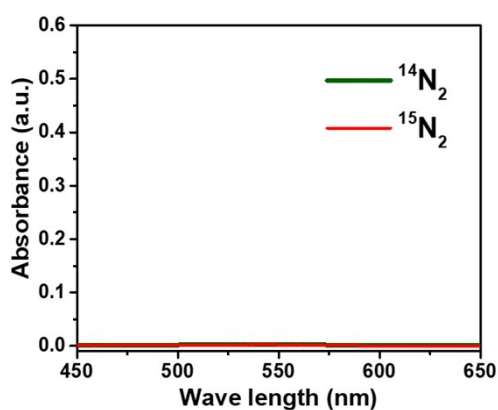


Figure S21. UV-vis spectra for determining the possible NO_2^- contamination from the feeding N_2 gas.

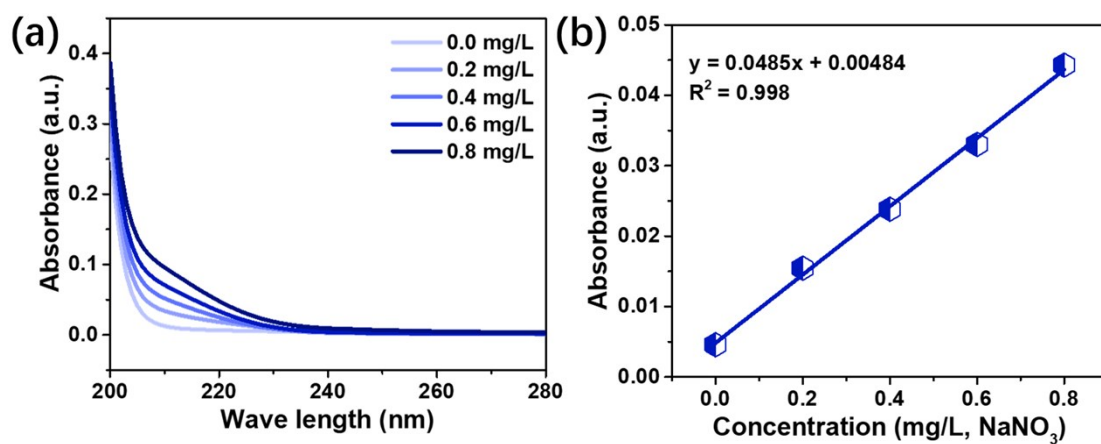


Figure S22. Calibration for nitrate determination. (a) UV-vis spectra for various concentrations of NaNO_3 . (b) Calibration curve used for calculating the concentration of nitrate.

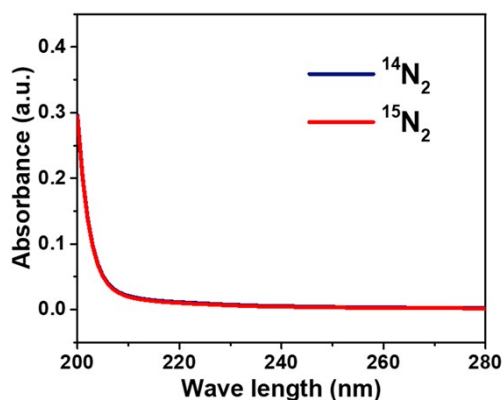


Figure S23. UV-vis spectra for determining the possible NO_3^- contamination from the feeding N_2 gas.

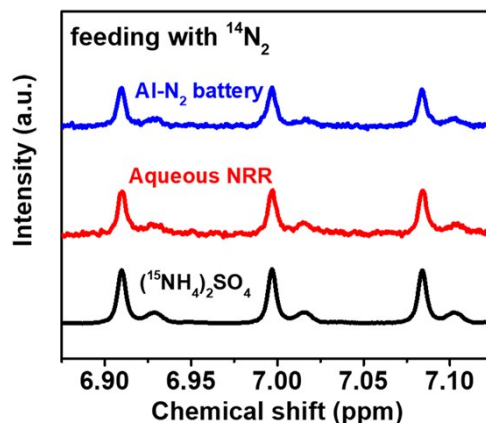


Figure S24. ^1H NMR spectra obtained by using $^{14}\text{N}_2$ as feeding gas and the standard $(^{14}\text{NH}_4)_2\text{SO}_4$.

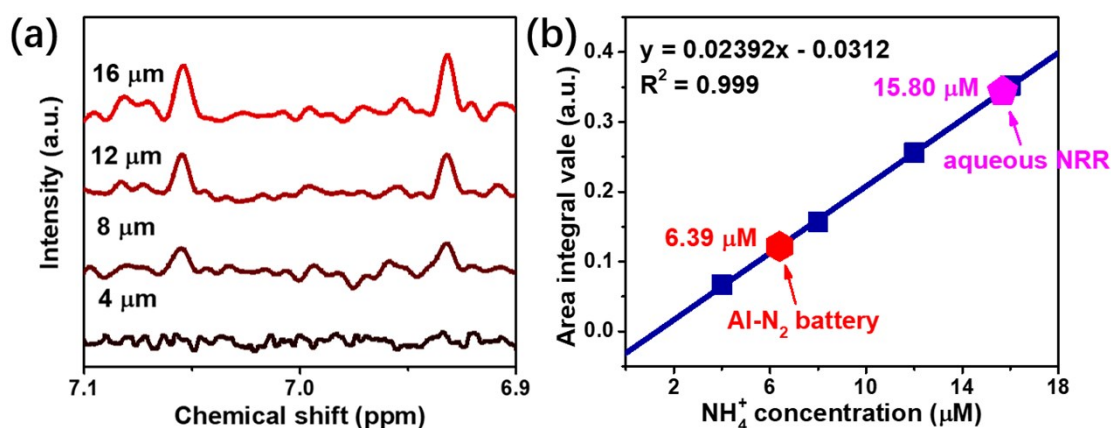


Figure S25. ^1H NMR spectra (a) and calibration curve (b) for the $^{15}\text{NH}_4^+$ standard samples with the various concentrations. It should be noted that, as described in experiment section, the volumes of electrolytes based on the hydrolysis of the cathodic AlN product and the aqueous electrolyte of 0.05 M H_2SO_4 are 200 mL and 40 mL,

respectively. Thereby, their NH_3 yields are
$$\frac{200 \text{ mL} \times 6.39 \mu\text{M} \times 17 \frac{\text{g}}{\text{mol}}}{0.4 \text{ mg} \times 2 \text{ h}} = 27.16$$

$$\text{mg/g}_{\text{cat}} \cdot \text{h} \text{ and } \frac{40 \text{ mL} \times 15.8 \mu\text{M} \times 17 \frac{\text{g}}{\text{mol}}}{0.4 \text{ mg} \times 2 \text{ h}} = 13.43 \text{ mg/g}_{\text{cat}} \cdot \text{h}, \text{ respectively.}$$

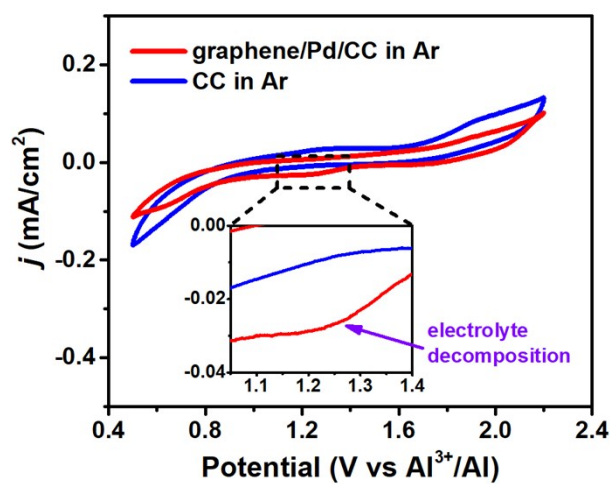


Figure S26. CV curves of the Al-N₂ battery with the CC electrode and the graphene/Pd/CC electrode at a scan rate of 0.05 mV/s in the Ar atmosphere.

Table S1. Data for several electrochemical reactions that form the basis of energy-storage devices.

Battery type	Chemical reaction equation	ΔG (kJ/mol)	Theoretical cell voltage (V)	Standard reduction potentials at 25°C	
				Reduction half-reaction	E° (V vs RHE)
Li-O ₂	2Li(s) + O ₂ (g) = Li ₂ O ₂ (s)	-606.1	3.10 ^{1, 2}	Li ⁺ (aq) + e ⁻ → Li(s)	-3.04
	4 Li(s) + O ₂ (g) = 2 Li ₂ O(s)	-561.2	2.91 ^{1, 2}		
Na-O ₂	4 Na(s) + O ₂ (g) = 2 Na ₂ O(s)	-218.8	1.13 ^{3, 4}	Na ⁺ (aq) + e ⁻ → Na(s)	-2.71
	2 Na(s) + O ₂ (g) = 2 Na ₂ O ₂ (s)	-447.7	2.33 ^{3, 4}		
Mg-O ₂	2 Mg(s) + O ₂ (g) = 2 MgO(s)	-569.3	2.95 ⁵	Mg ²⁺ (aq) + 2 e ⁻ → Mg(s)	-2.37
Al-O ₂	6 Al(s) + 3 O ₂ (g) = 3 Al ₂ O ₃ (s)	-1582.3	2.73 ⁶	Al ³⁺ (aq) + e ⁻ → Al(s)	-1.66
Zn-O ₂	2 Zn(s) + O ₂ (g) = 2 ZnO(s)	-318.3	1.65 ⁷	Zn ²⁺ (aq) + e ⁻ → Zn(s)	-0.76
Li-N ₂	6 Li(s) + O ₂ (g) = 2 Li ₃ N(s)	-154	0.53 ⁸	Li ⁺ (aq) + e ⁻ → Li(s)	-3.04
Al-N ₂	2 Al(s) + N ₂ (g) = 2 AlN(s)	-287	0.99	Al ³⁺ (aq) + e ⁻ → Al(s)	-1.66

These data suggest that a lower E° does not certainly result in a higher theoretical cell voltage. For instance, metallic Mg has a higher E° of -2.37 V than that of metallic Na, but the Mg-O₂ battery has a higher theoretical cell voltage of 2.95 V than that of Na-O₂ battery, so do Al-O₂ battery and Na-O₂ battery. This is attributed to the chemical stability of the discharged product because both $\Delta G(\text{Al}_2\text{O}_3)$ of -1582.3 kJ/mol and $\Delta G(\text{MgO})$

of -569.3 kJ/mol are much lower than those of Na_2O and Na_2O_2 . It should be noted that, taking an accounting of metals, more reactive metal (typically indicated by E°) is not the prerequisite for the formation of a more stable metal compound. Typically, metallic Li has much higher reactivity than metallic Al, but Al_2O_3 is much stable than Li_2O (indicated by ΔG). In the Al- N_2 battery system, the discharged AlN product has much lower $\Delta G(\text{AlN})$ of -287 kJ/mol than that of Li_3N ($\Delta G(\text{Li}_3\text{N}) = -154$ kJ/mol that implies its higher chemical stability than Li_3N , and, therefore, Al- N_2 battery exhibits a higher theoretical cell voltage and a higher spontaneity than the Li- N_3 battery, meanwhile metallic Al is more chemically stable than metallic Li under ambient conditions.

Table S2. Comparison of FEs based on Al-N₂ battery with the reported catalysts based on the electrochemical N₂ fixation in aqueous solution.

Catalyst	Electrolyte	FE/%	Reference
Graphene/Pd	Ionic liquid	51.2	This work
Au ₁ /C ₃ N ₄	0.005 M H ₂ SO ₄	11.1	Sci. Bull. 2018, 63, 1246
Au nanorods	0.1 M KOH	4.02	Adv. Mater. 2017, 29 , 1604799
AuPdP nanowires	0.1 M Na ₂ SO ₄	15.4	ACS Sustainable Chem. Eng. 2019, 7, 15772
Au@ZIF8	0.1 M Na ₂ SO ₄	44	Angew. Chem. Ed. Int. 2019, 131, 1
Au/N-carbon	0.1 M HCl	12.3	Small Methods 2018, 2, 1800202
Au/Ti ₃ C ₂	0.1 M HCl	18.34	ACS Appl. Mater. Interfaces 2019, 11, 25758
Au/CeOx/C	0.1 M HCl	10.1	Adv. Mater. 2017, 29, 1700001
Au/TiO ₂	0.1 M HCl	8.11	Adv. Mater, 2017 29, 1606550
Au flower	0.1 M HCl	6.05	ChemSusChem 2018, 11, 3480
Au ₆ /Ni	0.05 M H ₂ SO ₄	67.8	J. Am. Chem. Soc. 2019, 141, 14976
Pd/Cu/rGO	0.1 M KOH	4.3(0.1)	Adv. Energy Mater. 2018, 8, 1800124.
PdRu BPNs	0.1 M HCl	1.53	ACS Sustainable Chem. Eng. 2019, 7, 2400
Pd ₃ Cu ₁ alloy	1 M KOH	1.22	Nano Energy 58 (2019) 834
PdRu tripods	0.1 M KOH	1.85	J. Mater. Chem. A, 2019, 7, 801

Pt ₉₃ Ir ₇ alloy	0.001 M HCl	40.8	Chem. Commun., 2019, 55, 9335
Rh nanosheets	0.1 M KOH	0.217	J. Mater. Chem. A, 2018, 6, 3211
Ru _{as} /N-C	0.05 M H ₂ SO ₄	29.6	Adv. Mater. 2018, 30, 1803498
Ru _{sa} /ZrO ₂	0.1 M HCl	21	Chem, 2019, 5, 204–214
Ru-MoS ₂	0.01 M HCl	17.6	ACS Energy Lett. 2019, 4, 430
Bi NCs	0.5 M K ₂ SO ₄	66	Nat. Catal.,2019, 2, 448
BiVO ₄	0.2 M Na ₂ SO ₄	10.04	Small Methods 2019, 3, 1800333
Bi nanosheets	0.1 M Na ₂ SO ₄	10.46	ACS Catal. 2019, 9, 2902
CeO ₂ nanorods	0.1 M Na ₂ SO ₄	3.7	ACS Sustainable Chem. Eng. 2019, 7, 2889
Cr-CeO ₂	0.1 M Na ₂ SO ₄	3.84	Inorg. Chem. 2019, 58, 5423
Cr ₂ O ₃ nanofiber	0.1 M HCl	8.56	Chem. Commun., 2018, 54, 12848
Cr ₂ O ₃ NPs/rGO	0.1 M HCl	7.33	Inorg. Chem. 2019, 58, 2257
hollow Cr ₂ O ₃	0.1 M Na ₂ SO ₄	6.78	ACS Catal. 2018, 8, 8540
Fe/Fe ₂ O ₄	0.1 M PBS	8.29	ACS Catal. 2018, 8, 9312
Fe ₃ O ₄ nanorod	0.1 M Na ₂ SO ₄	2.6	Nanoscale, 2018, 10, 14386
Fe ₃ S ₄	0.1 M HCl	6.45	Chem. Commun., 2018, 54, 13010
γ-Fe ₂ O ₃	0.1 M HCl	12.28	ACS Sustainable Chem. Eng. 2019, 7, 8853

Fe-N/C	0.1 M KOH	56.55	Nature Commun.2019, 10,341
single Fe atom	0.1 M PBS	16.8	Nano Energy, 2019, 61, 420
FeS@MoS ₂ /CFC	0.1 M Na ₂ SO ₄	2.96	Nano Energy, 2019, 62, 282
Fe-N/C	0.1 M KOH	9.28	ACS Catal. 2019, 9, 336
CoFe ₂ O ₄ /graphene	0.1 M Na ₂ SO ₄	6.2	Chem. Commun., 2019, 55, 12184

Reference

1. P. G. Bruce, S. A. Freunberger, L. J. Hardwick and J.-M. Tarascon, *Nat. Mater.*, 2012, **11**, 19-29.
2. L. Johnson, C. Li, Z. Liu, Y. Chen, S. A. Freunberger, P. C. Ashok, B. B. Praveen, K. Dholakia, J.-M. Tarascon and P. G. Bruce, *Nat. Chem.*, 2014, **6**, 1091-1099.
3. J.-l. Ma, N. Li, Q. Zhang, X.-b. Zhang, J. Wang, K. Li, X.-f. Hao and J.-m. Yan, *Energy Environ. Sci.*, 2018, **11**, 2833-2838.
4. S. Kang, Y. Mo, S. P. Ong and G. Ceder, *Nano Letters*, 2014, **14**, 1016-1020.
5. Q. Dong, X. Yao, J. Luo, X. Zhang, H. Hwang and D. Wang, *Chem. Commun.*, 2016, **52**, 13753-13756.
6. S. Yang and H. Knickle, *J. Power Sources*, 2002, **112**, 162-173.
7. F. Cheng and J. Chen, *Chem. Soc. Rev.*, 2012, **41**, 2172-2192.
8. A. J. Martín, T. Shinagawa and J. Pérez-Ramírez, *Chem*, 2019, **5**, 263-283.